Pressure distribution and aerodynamic forces on stationary box bridge sections

Francesco Ricciardelli[†]

Department of Mechanics and Materials, University of Reggio Calabria, Via Graziella, Feo di Vito, 89060 Reggio Calabria, Italy

Horia Hangan[‡]

The Boundary Layer Wind Tunnel Laboratory, The University of Western Ontario, London, Ontario, N6A 5B9, Canada

Abstract. Simultaneous pressure and force measurements have been conducted on a stationary box deck section model for two configurations (namely without and with New Jersey traffic barriers) at various angles of incidence. The mean and fluctuating aerodynamic coefficients and pressure coefficients were derived, together with their spectra and with the coherence functions between the pressures and the total aerodynamic forces. The mean aerodynamic coefficients derived from force measurements are first compared with those derived from the integration of the pressures on the deck surface. Correlation between forces and local pressures are determined in order to gain insight on the wind excitation mechanism. The influence of the angle of incidence on the pressure distribution and on the fluctuating forces is also analysed. It is evidenced how particular deck section areas are more responsible for the aerodynamic excitation of the deck.

Key words: bridge aerodynamics; aerodynamic forces; wind tunnel testing; pressure measurement.

1. Introduction

The design of cable supported bridges usually involves wind tunnel testing on section models to assess the wind loads and to check the aerodynamic stability of the deck section. These tests include two stages: (i) firstly the total aerodynamic forces are measured on the fixed model to evaluate the stationary aerodynamic coefficients and (ii) secondly the accelerations and/or the displacements are measured on a spring mounted model, for different wind speeds to check the aerodynamic stability. In addition, the flutter derivatives can be evaluated by either measuring the aerodynamic forces on the model driven into a sinusoidal motion, or by measuring the free oscillation of the model at different wind speeds.

The static and dynamic forces on the stationary model are usually measured using load cells. An alternative approach is that of measuring the instantaneous pressure distribution on the deck, and calculating the time histories of the aerodynamic forces by space integration of the pressure

---

† Assistant Professor
‡ Assistant Professor and Associate Research Director

distribution. The latter technique is very seldom used, but quite attractive due to the possibility of having (i) a more accurate frequency domain description of the fluctuating section forces, (ii) information about the mean and fluctuating pressure distribution on the bridge deck section and (iii) a measurement of the spanwise coherence of the fluctuating forces (Larose 1992, Larose *et al.* 1998, Haan *et al.* 2000). The high performance of high speed pressure scanning systems allow for simultaneous pressure measurement at a sufficiently high rate (say 200 to 400 Hz) at a large number of locations (say 10 sections with 24 taps each). The additional cost with respect to the traditional approach using load cells is reasonable, and is mainly related to a higher cost for the pressure model.

In dynamic tests, the use of a pressure model also allows for simultaneous measurement of aerodynamic forces and structural response which, to the authors' knowledge, has to date never been undertaken. Though redundant from the design point of view, this technique allows to derive information about the mechanism of the wind excitation, to be eventually used to modify the aerodynamics of the cross section or to implement aerodynamic control.

Based on these ideas, a research program has been started as a co-operation between the *Boundary Layer Wind Tunnel Laboratory* of the *University of Western Ontario* and the *University of Reggio Calabria*, aiming at :

   a. developing new experimental techniques for the evaluation of the aerodynamic characteristics of long span bridge box decks through pressure measurements;
   b. analysing the mechanism of the flow induced excitation of long span bridge box decks.

The program is part of a larger project aimed also at (i) exploring the possibility of evaluating the aerodynamic characteristics of box bridge decks using Computational Fluid Dynamics techniques and (ii) investigating aerodynamic control strategies for long span bridge decks. As a first stage, static and dynamic wind tunnel tests have been carried out on the section model of the new Sunshine Skyway Bridge, Tampa, Florida. The tests were aimed at analysing the nature of the aerodynamic forces by studying the correlation between the total forces, the local pressures, the dynamic response and the characteristics of the wake flow, as well as at calibrating new techniques for the evaluation of the aerodynamic parameters based on the use of high speed pressure scanning systems. This paper reports the results of the static tests.

2. Wind tunnel tests

Static tests on a section model of the Sunshine Skyway Bridge were performed in smooth flow in BLWT I at the *Boundary Layer Wind Tunnel Laboratory*. The bridge is a 692 m long cable stayed bridge, with a main span of 364 m, a deck width and height of 28.60 m and 4.25 m respectively (Fig. 1). The 1:80 scaled, 2.12 m long pressure model is made of an aluminium core and a plywood skin (Figs. 2 and 3). Three PSI pressure transducers were located inside the model to reduce the tubing length. Twenty-four of the 48 pressure taps, the so called lift taps, were arranged in one section around midspan, such that the projected tributary area on the deck plane is constant (Figs. 4 and 5). This allows the total aerodynamic force orthogonal to the deck plane to be calculated by adding the pressure at the lift pressure taps. Similarly, the remaining 24 pressure taps, the so called torque taps, were arranged in one section about 5 cm away from the former, such that the product of the tributary area and the distance from the deck axis is constant. This allows the total torque to be calculated by adding the pressure at the torque pressure taps. The model was placed in a static rig equipped with 6 load cells, which allowed the measurement of the three
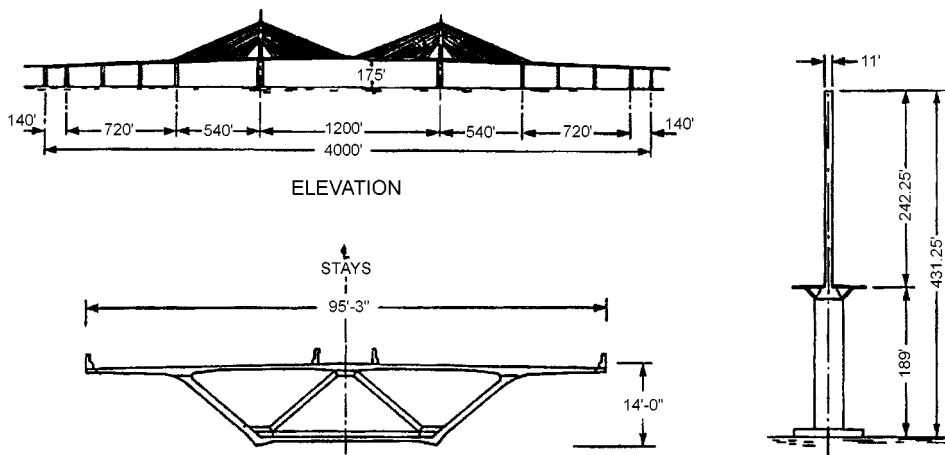
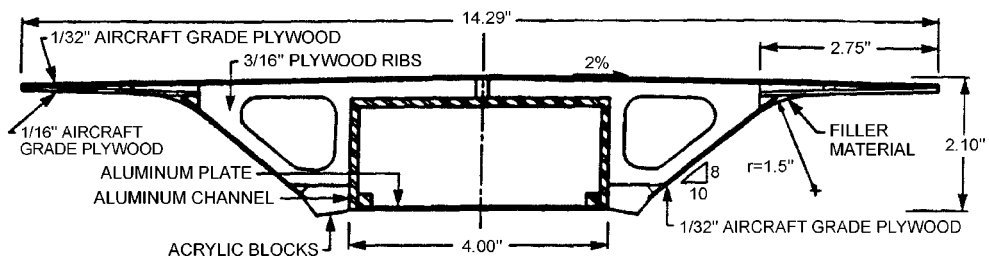Fig. 1 The new Sunshine Skyway Bridge (from Davenport and King 1982)

Fig. 2 Schematic of the section model (from Davenport and King 1982)
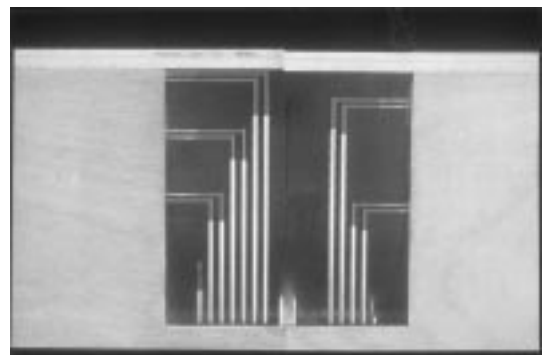

Fig. 3 Section model

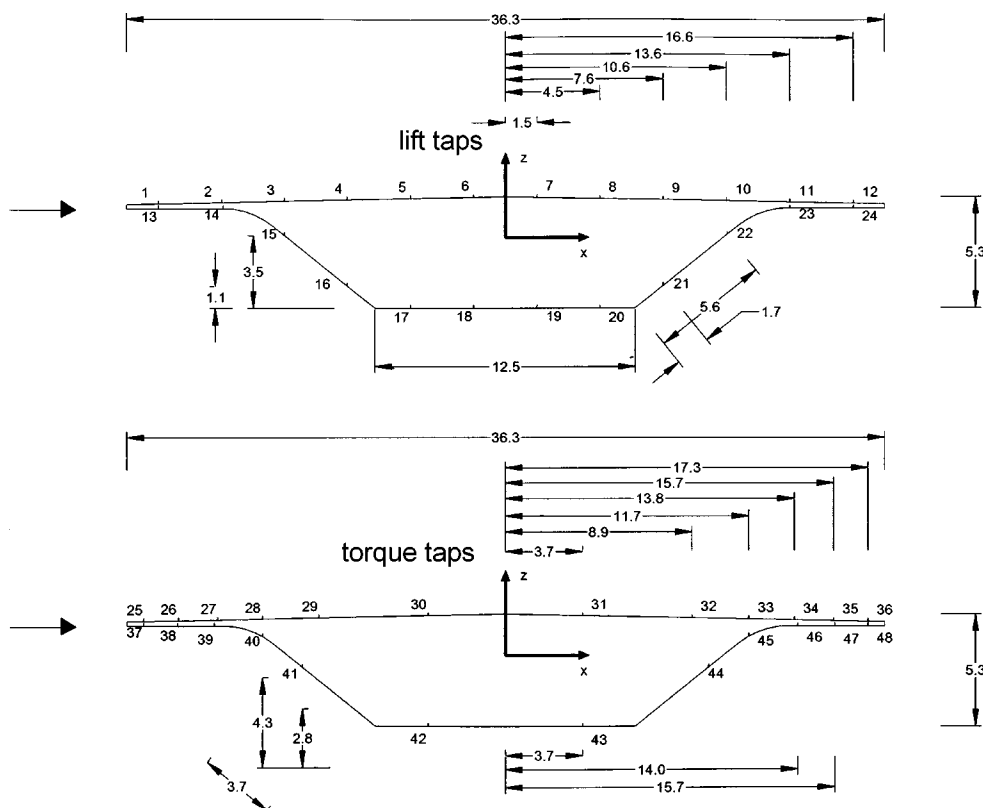Fig. 4 Pressure taps on the section model

Fig. 5 Positioning of the pressure taps (dimensions in cm)

Fig. 6 Wind tunnel setup

components of the total aerodynamic forces (Fig. 6). A cross hot wire anemometer was placed about 0.40 m downstream the trailing edge of the section to measure the wake turbulence components.

In the tests total aerodynamic forces, local pressures and wake wind velocities were measured simultaneously for 17 angles of incidence of 0°, $\pm 1^{\circ}$, $\pm 2^{\circ}$, $\pm 3^{\circ}$, $\pm 4^{\circ}$, $\pm 6^{\circ}$, $\pm 8^{\circ}$, $\pm 10^{\circ}$, $\pm 12^{\circ}$ (positive

angles nose up), 2 wind speeds of 9.8 m/s and 12.2 m/s, and 2 configurations, namely with and without New Jersey traffic barriers (as in Fig. 1). Measurements were taken at 400 Hz for 256 s.

3. Aerodynamic coefficients

In order to check the performance of the pressure model in the estimation of the aerodynamic forces, the static body-related aerodynamic coefficients evaluated from the pressure readings were compared to those measured from the load cells. The aerodynamic coefficients were evaluated from the load cells readings as :

$$C_x = \frac{F_{x1} + F_{x2}}{\frac{1}{2}\rho V^2 BL} \tag{1}$$

$$C_z = \frac{F_{z1} + F_{z2}}{\frac{1}{2}\rho V^2 BL} \tag{2}$$

$$C_M = \frac{M_1 + M_2}{\frac{1}{2}\rho V^2 B^2 L} \tag{3}$$

where F_{x1}, F_{x2}, F_{z1}, F_{z2} M_1 and M_2 are the forces in the x-direction, forces in the z-direction and torque measured at the far and near load cells, respectively, and where ρ is the air density, V is the tunnel speed and B and L are the model width and length.

From the pressure measurements the aerodynamic coefficients were calculated as :

$$C_x = \sum_{i=1}^{48} C_{pi} \cdot \alpha_i \tag{4}$$

$$C_z = a \cdot \sum_{i=1}^{24} C_{pi} \tag{5}$$

$$C_M = b \cdot \sum_{i=25}^{48} C_{pi} \tag{6}$$

where C_{pi} is the pressure coefficient at the i-th pressure tap (Fig. 5), α_i the x-direction component of the normal at the i-th pressure tap, and where a and b are coefficients accounting for the spacing between the taps.

Figs. 7 and 8 show the z-force (perpendicular to the deck plane, positive upward) and torque (positive clockwise) coefficients as a function of the angle of incidence. The agreement between the results obtained from the load cells measurements and from the integration of pressures is quite good, except for the z-force coefficient of the deck with traffic barriers, for which some discrepancies were found between the two results. This is believed to be mainly due to the contribution of the pressure acting on the barriers, which is not taken into account through the
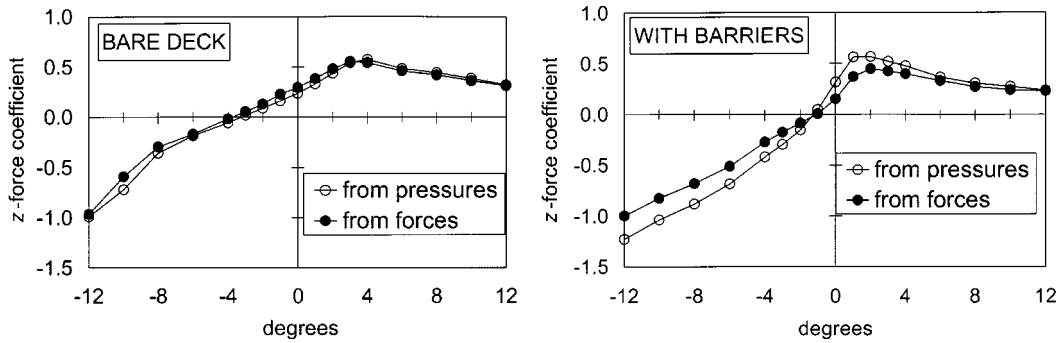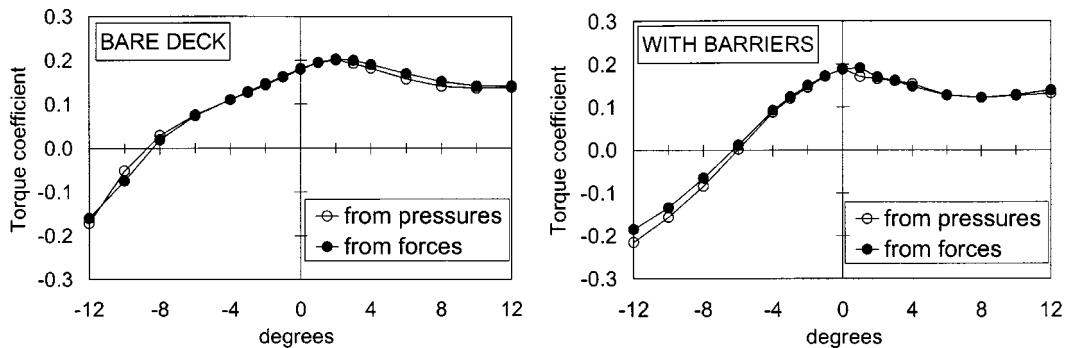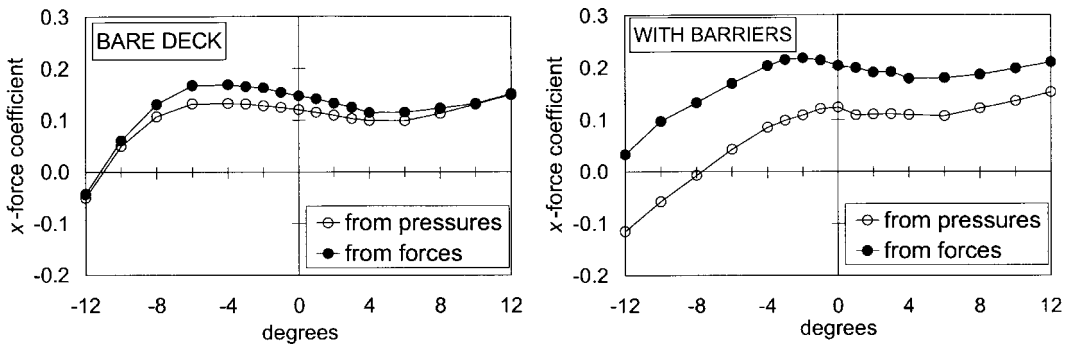
Fig. 7 *z*-force coefficient vs. angle of incidence

Fig. 8 Torque coefficient vs. angle of incidence

Fig. 9 *x*-force coefficient vs. angle of incidence

pressure measurement, as the barriers were not instrumented with pressure taps. This effect is even more pronounced in the case of the *x*-force (parallel to the deck plane, positive along wind) coefficient, shown in Fig. 9, where the difference between the results obtained from the pressure and force measurements gets quite large. In this case the contribution of the barriers is important, and if neglected will result in an underestimation of the total aerodynamic force. For the bare deck the discrepancies in the *x*-force coefficient are much lower (Fig. 9), and mainly due to the small number

of pressure taps contributing to the *x*-force, and to the contribution of friction forces, which is neglected when the force coefficient is derived from pressure measurements. Similar results were found by Larose (1992).

Globally the performance of the pressure model proves encouraging, though it is clear that a poor positioning of the pressure taps can lead to errors in the estimation of the total forces acting on the deck. However, if the pressure taps are properly positioned, only the friction forces are neglected, and the results are quite accurate.

4. Effect of the traffic barriers on the mean pressure distribution

The main advantages of taking pressure measurements instead of force measurements in static
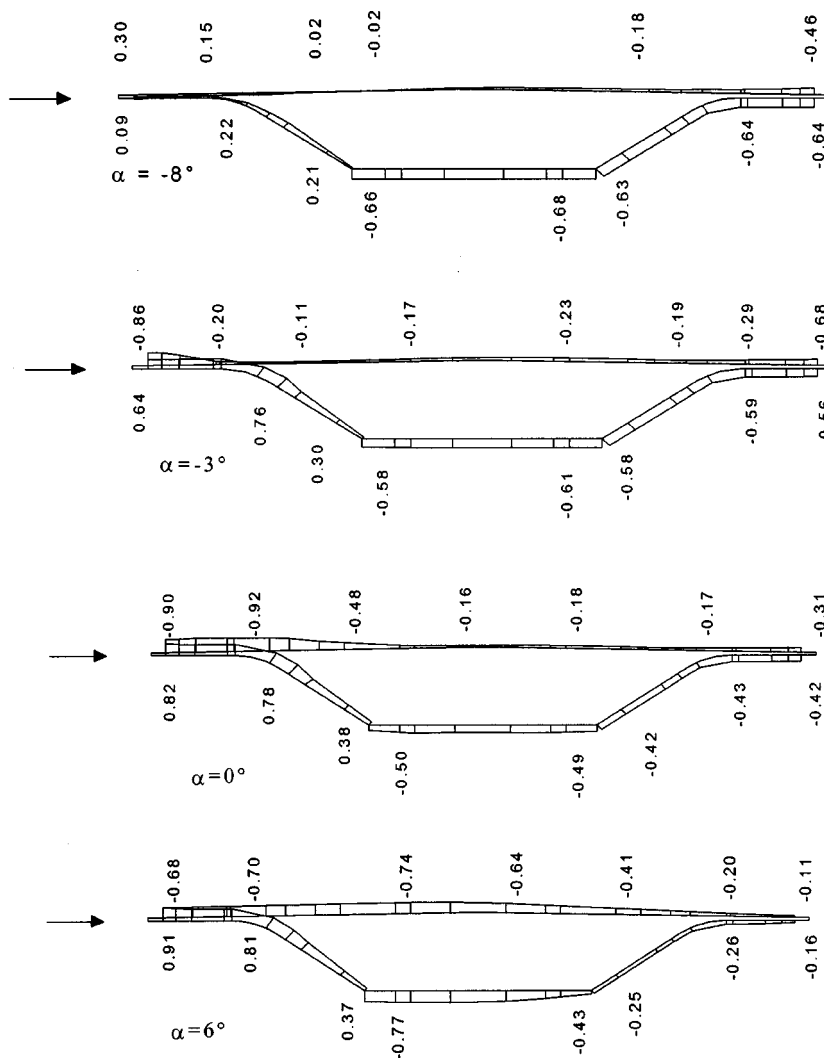
Fig. 10 Mean pressure coefficients on the bare deck

tests is related to the possibility of: (i) having a more accurate description of the fluctuating forces, and (ii) having a picture of the distribution of the mean and fluctuating pressure field on the deck, which allows a better understanding of the flow excitation mechanism. The analysis of the mean pressure distribution on the deck with varying angle of incidence, and in relation with the aerodynamic forces allows understanding the flow behaviour. In addition the comparison of the mean pressure distribution on the bare deck and that on the deck with traffic barriers allows understanding of the changes brought to the aerodynamics of the cross section by addition of the barriers.

As an example, in Fig. 10 the distribution of the mean pressures on the bare deck is reported for angles of incidence of -8°, -3°, 0° and +6°.

For an angle of incidence of -8° the values of the pressure coefficients on the upper face of the deck are low, positive towards the leading edge and negative towards the trailing edge. Also on the lower upstream portion of the deck the pressure coefficients have low positive values, while the remaining part of the lower face of the deck has an almost constant value of the pressure coefficient of about -0.65. This indicates that there is no marked flow separation on the upper face of the deck, while on the lower face separation takes place from the upstream edge of the lower slab.

For an angle of incidence of -3° the flow separation occurs at the leading edge, and probably towards the trailing edge, on the upper face of the deck, with low negative values of the pressure coefficients in between, indicating a possible smooth reattachment. On the lower face separation takes again place from the upstream edge of the lower slab, but in this case the positive pressure acting on the lower upstream portion of the deck is larger. This results in balancing the negative pressure acting on the lower downstream portion of the deck, hence reducing the total lift force ($C_z = -0.30$ for $\alpha = -8°$ and $C_z = -0.05$ for $\alpha = -3°$). However, the upstream positive pressure and the downstream negative pressure act as a couple, increasing the total torque ($C_M = 0.03$ for $\alpha = -8°$ and $C_M = 0.13$ for $\alpha = -3°$).

For angles of incidence of 0° and +6°, the flow separates from the upper face of the deck at the leading edge, with limit reattachment towards the trailing edge, resulting in negative pressure coefficients on the entire upper face of the deck. This negative pressure distribution is responsible
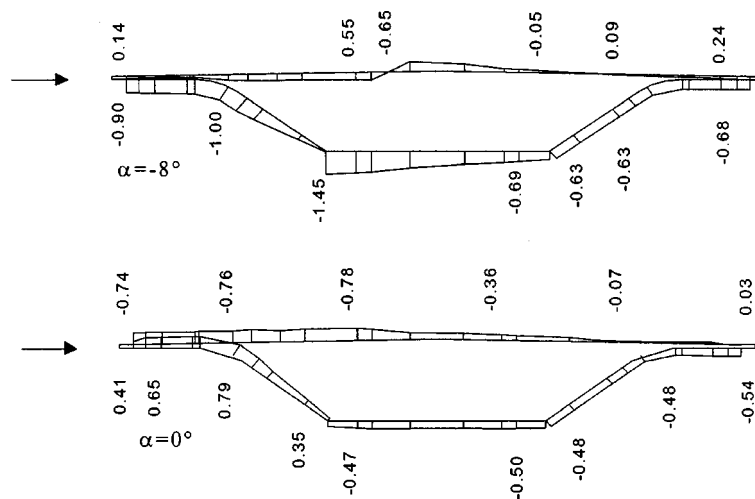

Fig. 11 Mean pressure coefficients on the deck with traffic barriers

for the large positive lift force acting on the deck with positive angles of incidence ($C_z = +0.45$ for $\alpha = +6°$).

When the traffic barriers are added to the deck, the pressure distribution completely changes, not only on the upper face, where the barriers are located, but also on the lower face. This indicates that in such cases the addition of the barriers does not result in a local change in the flow pattern, but rather in a modification of the global aerodynamics of the cross-section.

As an example, in Fig. 11 the mean pressure distribution on the deck with traffic barriers is shown, for angles of incidence of -8° and 0°, for comparison with those of Fig. 10. Though the pressure distribution for an angle of incidence of 0° is almost similar to that of the bare deck, in the case of an angle of incidence of -8° the pressure distribution is strongly modified by the presence of the barriers. On the upstream part of the upper face of the deck the pressure is positive, as in the case of the bare deck, but with larger pressure coefficients. The flow, however, separates from the central traffic barrier causing a region of negative pressures around the centreline of the deck. The main differences in the pressure distribution, however, are in the lower part of the deck. Due to the presence of the upstream barrier, the flow separates from the lower face of the deck at the leading edge, causing in the upstream portion of the deck negative pressure coefficients as high as -1.00. A second separation takes place from the upstream edge of the lower slab, where a negative pressure coefficient as high as -1.45 was measured. The large negative pressure acting on the lower face of the deck results in a large negative lift force ($C_z = -0.88$) and in a moderate negative torque ($C_M = -0.08$).

For angles of incidence larger than 4° the mean pressure distribution tends to be the same in the two configurations. This occurs because for positive angles of incidence the upper portion of the deck is in a wake flow and the traffic barriers have a limited effect on the aerodynamics of the section.

The differences in the flow pattern, and therefore in the aerodynamic coefficients, between the case of the bare deck and that of the deck with traffic barriers are responsible for a different aeroelastic behaviour of the section in the two configurations. A deeper insight into the effect on the aeroelastic behaviour of the changes in the pressure distribution will be possible with the analysis of the variation of the pressure distribution on the aeroelastic model with varying wind velocity.

5. Fluctuating aerodynamic forces

In Fig. 12 RMS torque coefficient is plotted as a function of the angle of incidence for the bare
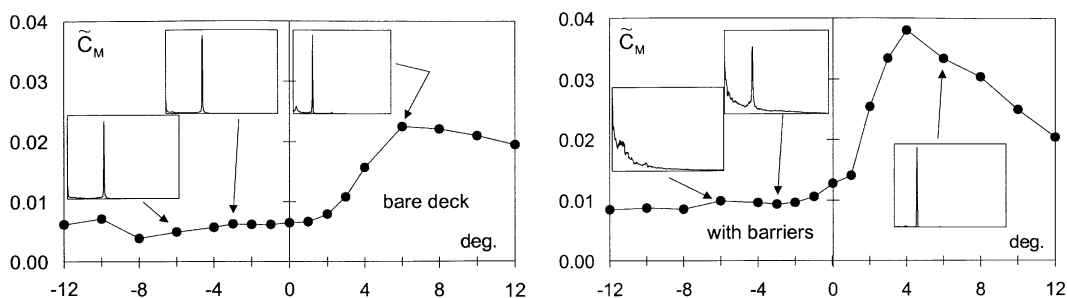

Fig. 12 RMS torque coefficient vs. angle of incidence

deck and for the deck with traffic barriers. In the plots the Power Spectra of the torque coefficient for angles of incidence of -6°, -3° and 6° are also shown. For positive angles of incidence the fluctuating torque on the deck with traffic barriers can be as much as twice that on the bare deck. The spectra of the torque coefficient show that this is associated to a change, with varying angle of incidence, in the magnitude of the shedding induced forces. In the case of the bare deck, independently of the angle of incidence vortex shedding is responsible for almost all the fluctuating torque, and variations in the RMS torque coefficient are mainly associated with variations in the magnitude of the spectral peak. However, for the deck with traffic barriers, while for negative angles of incidence most of the torque comes from low frequency components, for positive angle of incidence a narrow and powerful peak appears on the spectrum, indicating a strong increase in the fluctuating torque associated with vortex shedding.

The variation of the Strouhal number with the angle of incidence for the two configurations also confirms that for angles of incidence smaller than 3° the section behaves differently in the two configurations, but for larger angles of incidence the behaviour is the same. In Fig. 13 the Strouhal number (evaluated assuming the width of the deck as reference length) for the section in the two configurations is plotted as a function of the angle of incidence. It is evident that vortex shedding occurs at different frequencies (and eventually does not occur regularly) in the two configurations when the angle of incidence is smaller than 3°. It instead occurs at a constant frequency corresponding to $St = 0.59$ for both configurations and independently of the angle of incidence, when this is larger
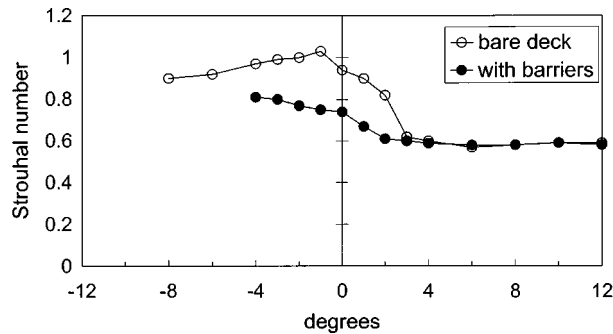

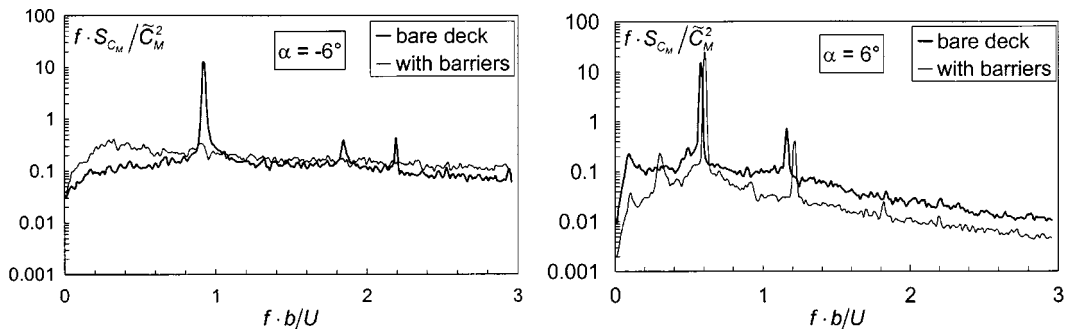Fig. 13 Strouhal number vs. angle of incidence

Fig. 14 Spectra of the torque coefficient

than 3°. In Fig. 14 the spectra of the torque coefficient are plotted for the two configurations and for angles of incidence of -6° and +6° respectively. For $\alpha = +6°$ the two spectra look quite similar, with a minor difference in the shedding frequency. For $\alpha = -6°$, however, the spectrum in the configuration with barriers does not show a regular vortex shedding as it occurs for the case of the bare deck.

6. Fluctuating pressure distribution

The analysis of the distribution of the deck fluctuating pressures allows some insight into the mechanism of wind excitation of the bridge.

In Fig. 15 the distribution of the RMS pressure coefficients on the bare deck is shown for an angle of incidence of 0°, together with the Power Spectra of the pressure at four locations on the deck. The figure shows that most of the dynamic excitation comes from two areas: the area around the trailing edge of the deck and an area about one quarter of the deck width downstream the leading edge, the latter corresponding to the reattachment of the separated flow. The pressure fluctuations acting on the trailing edge are mainly associated with vortex shedding, and their spectra have a narrow peak centred at the shedding frequency. Conversely, the pressure fluctuations on the upstream part of the deck are associated with flow reattachment, and their energy is distributed over a broad range of frequencies. This suggests that the pressure fluctuations at the trailing edge are more effective in contributing to the total fluctuating aerodynamic forces.

To confirm that, in Fig. 16 the distribution of the RMS pressure coefficients is again shown, together with the coherence functions of the pressure and the total torque, at four locations on the
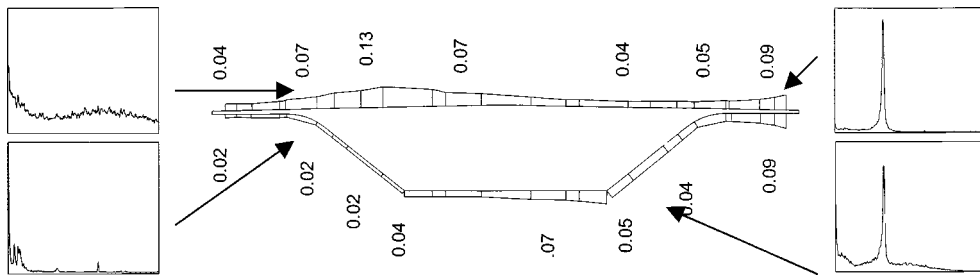

Fig. 15 RMS pressure coefficients and pressure spectra on the bare deck ($\alpha = 0^o$)

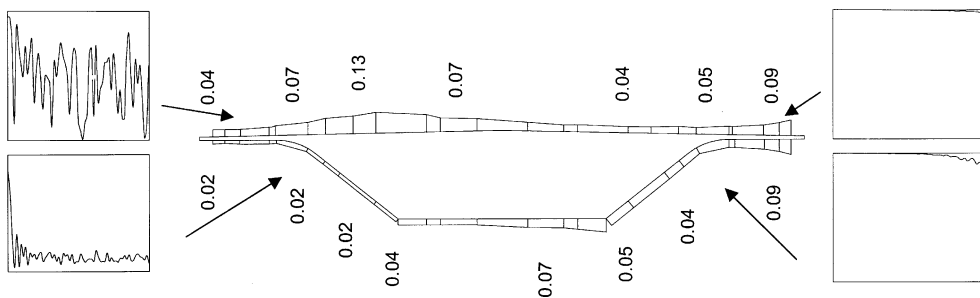

Fig. 16 RMS pressure coefficients and pressure-torque coherence on the bare deck ($\alpha = 0^o$)

deck. The pressures in the area around the trailing edge of the deck are fully coherent with the torque in the entire range of frequencies of interest, which confirms the effectiveness of the pressure fluctuations in that area in contributing to the total torque. However, the coherence between the pressures fluctuations on the upstream portion of the deck and the torque is almost low, which confirms their low contribution to the total excitation of the deck.

In Fig. 17 the RMS pressure coefficients of the deck with traffic barriers are shown, together with the spectra of the pressure fluctuations at four locations on the deck. The pressure fluctuations are generally larger in this case, but again the largest values occur in the downstream part of the deck, with RMS pressure coefficients as high as 0.17. As for the bare deck, the pressure fluctuations in the downstream part of the deck are associated with vortex shedding, having a spectrum with a narrow peak at the shedding frequency and a full coherence with the total torque. The pressure fluctuations on the upstream part of the deck are associated with flow reattachment, showing a broad banded spectrum and low values of the coherence with torque.
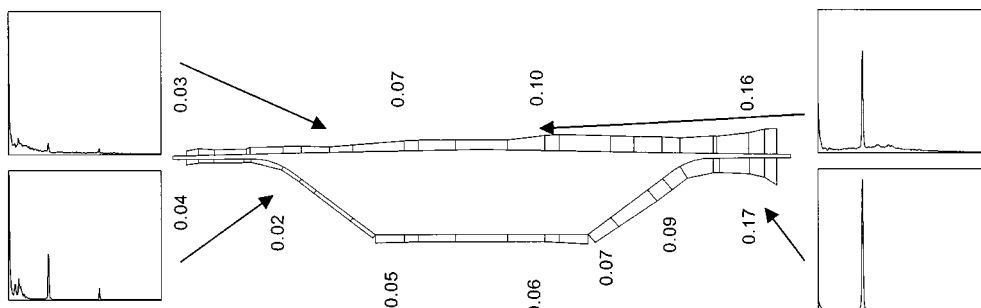

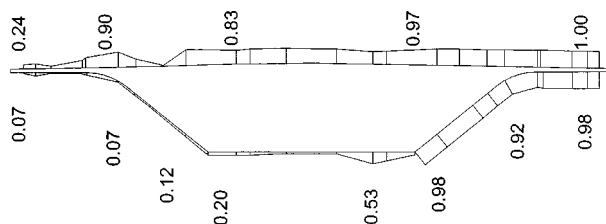Fig. 17 RMS pressure coefficients and pressure spectra on the deck with barriers ($\alpha = 0^o$)

Fig. 18 Coherence of pressures and torque at the shedding frequency (bare deck, $\alpha = 0^o$)
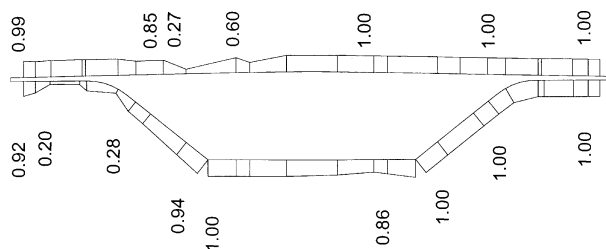

Fig. 19 Coherence of pressures and torque at the shedding frequency (with barriers, $\alpha = 0^o$)

The correlation between the pressure fluctuations and the torque is summarised in Figs. 18 and 19, where the distribution of the values of the coherence function of local pressures and torque at the shedding frequency is shown. In the case of the bare deck (Fig. 18) large values of the coherence occur on the upper face of the deck (except for points close to the leading edge), and on the downstream part of the lower face of the deck. For the deck with traffic barriers (Fig. 19) the coherence is full at almost all locations on the deck, indicating a more efficient mechanism of excitation.

As far as the correlation between the local pressures and the *z*-forces is concerned, similar results were found, with areas that contribute to the lift excitation more than others. However for the particular bridge chosen the torsional behaviour is dominant (dynamic tests showed torsional shedding induced response and torsional flutter), and therefore only the results related to torque were shown.

The coherence with the *x*-force was instead not analysed because of the mentioned poor accuracy of the latter as evaluated from the pressure readings.

The characteristics of the fluctuating pressures on the bridge deck pointed out in this section are those relative to a stationary model, and are subject to changes as the model starts to oscillate. This latter case will be investigated through dynamic tests.

6. Conclusions

The possibility of using pressure tests for the evaluation of stationary aerodynamic characteristics of long span bridge box decks was investigated here.

It was shown that pressure measurements, made through high speed pressure scanning systems allow an accurate estimation of the stationary aerodynamic coefficients, provided that the pressure taps are properly located on the cross-section.

The advantages of pressure measurements over force measurements are in an accurate description of the fluctuating forces over a broad frequency range, and in the availability of the mean and fluctuating pressure distributions on the deck. These information can be used to better understand the mechanism of the aerodynamic excitation of the deck, and, in the design stage, to help modifying the cross-section aerodynamics in order to obtain a better performance.

For the particular bridge considered it was found that most part of the dynamic excitation is associated with the action of the pressures fluctuations induced by vortex shedding towards the deck trailing edge.

Two configurations, the bare deck and the deck with New Jersey traffic barriers, were analysed. The addition of the traffic barriers resulted in a modification of the global aerodynamics of the section, rather than in a local modification of the flow in vicinity of the barriers. The fluctuating aerodynamic forces for the traffic barriers case are larger than for the bare deck case. This results from larger components of the pressure fluctuations at the shedding frequency and from a higher coherence between the local pressures and the total aerodynamic forces.

References

Davenport, A.G. and King, J.P.C. (1982), "A study of the wind effect for the Sunshine Skyway Bridge, Tampa, Florida, concrete alternate", *BLWT-SS24-1982*, The Boundary Layer Wind Tunnel Laboratory, The University of Western Ontario, London, Canada.
Hann, F.L. jr., Kareem, A. and Szewczyk, A.A. (2000), "Experimental measurements of spanwise correlation of

self-excited forces on a rectangular cross section", *Proc. of Fourth Int. Colloquium on Bluff Body Aerodynamic and Applications*, Bochum, Germany

Larose, G.L. (1992), "The response of a suspension bridge deck to turbulent wind: the taut strip model approach", MESc Thesis, The Boundary Layer Wind Tunnel Laboratory, The University of Western Ontario, London, Canada.

Larose, G.L., Tanaka, H., Gimsing, N.J. and Dyrbye, C. (1998), "Direct measurements of buffeting wind forces on bridge decks", *J. Wind Eng. Ind. Aerod.*, **74-76**, 809-818.

GS